

Supplement of Atmos. Chem. Phys., 16, 8609–8642, 2016  
<http://www.atmos-chem-phys.net/16/8609/2016/>  
doi:10.5194/acp-16-8609-2016-supplement  
© Author(s) 2016. CC Attribution 3.0 License.



*Supplement of*

## **Mediterranean intense desert dust outbreaks and their vertical structure based on remote sensing data**

**Antonis Gkikas et al.**

*Correspondence to:* Antonis Gkikas (antonis.gkikas@bsc.es)

The copyright of individual parts of the supplement might differ from the CC-BY 3.0 licence.

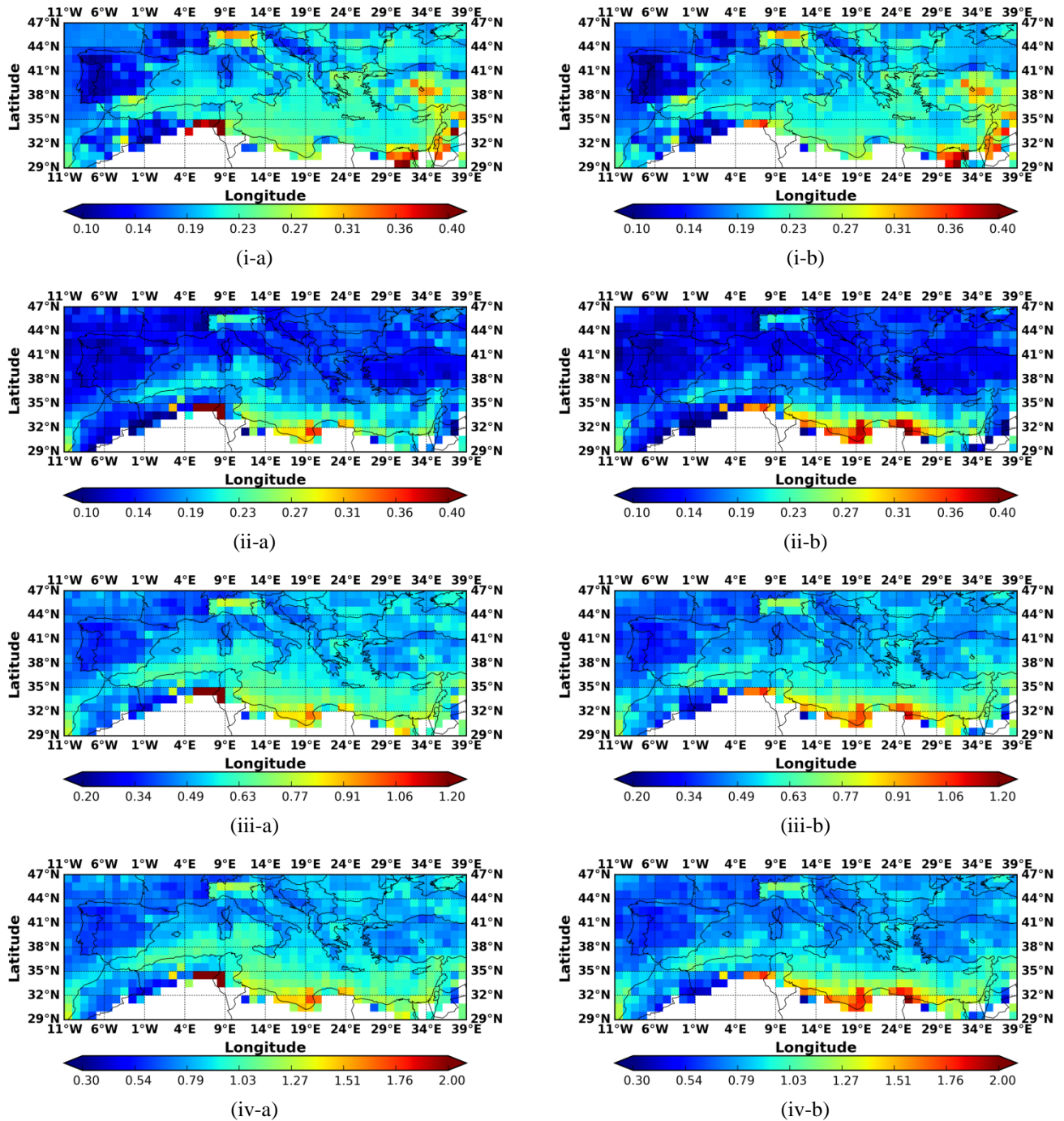


**Figure S1:** Geographical distributions of: (i) the long-term averaged AOD at 550 nm, (ii) the associated standard deviation, (iii) the strong ( $Mean + 2*Std$ ) and (iv) the extreme ( $Mean + 4*Std$ ) thresholds, over the broader Mediterranean basin, calculated for the periods: (a) 1 Mar. 2000 - 28 Feb. 2013 (MODIS-Terra) and (b) 2003 - 2012 (MODIS-Aqua). White pixels correspond to areas with AOD retrievals' availability lower than 5%.

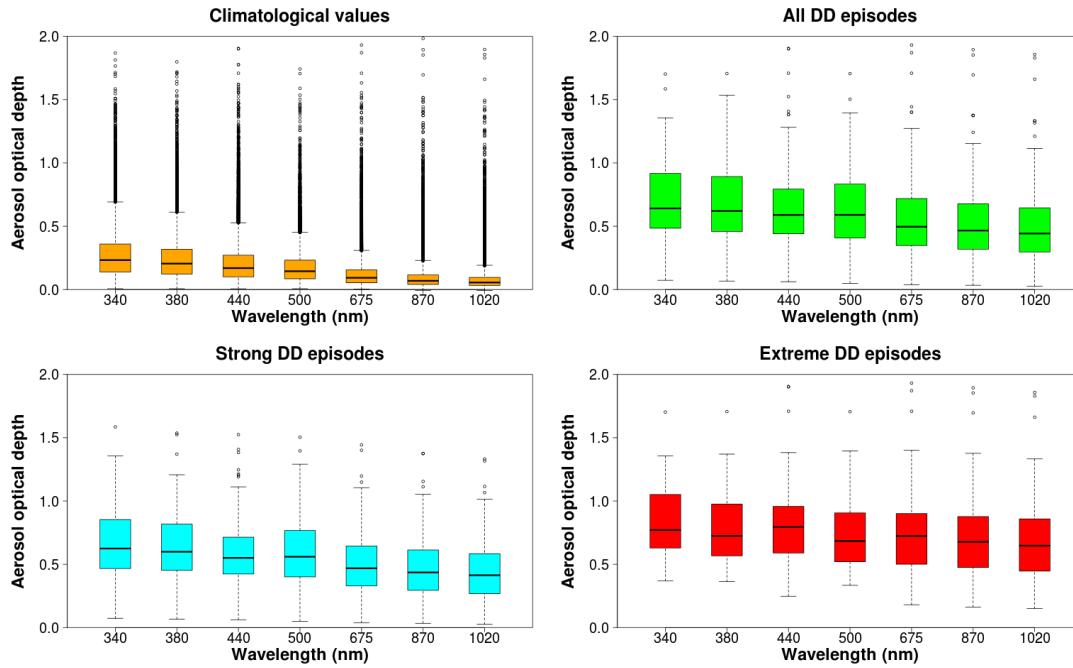
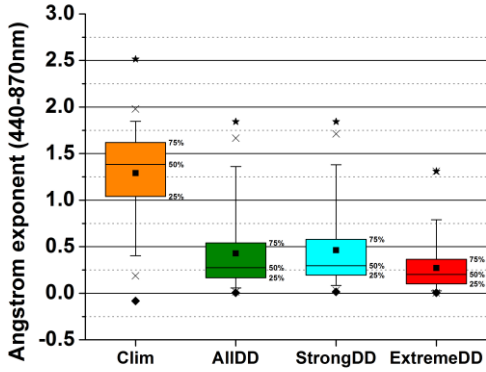
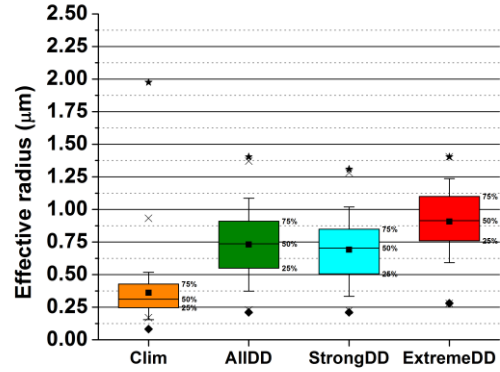


**Figure S2:** Spectral variation of the climatological AERONET *AOD* retrievals (orange, N=54147) as well as their corresponding values for the overall intense (green, N=346), strong (cyan, N=283) and extreme (red, N=63) *DD* episodes, which have been identified by the satellite algorithm.

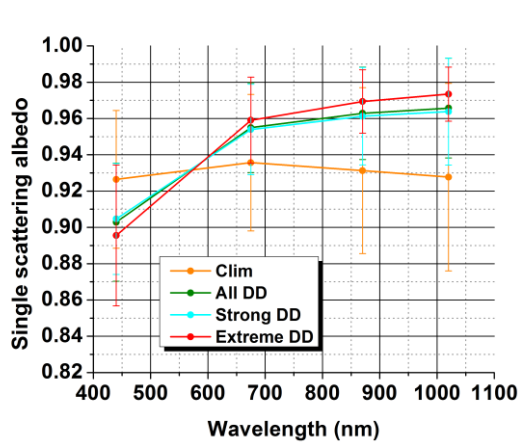


(i)

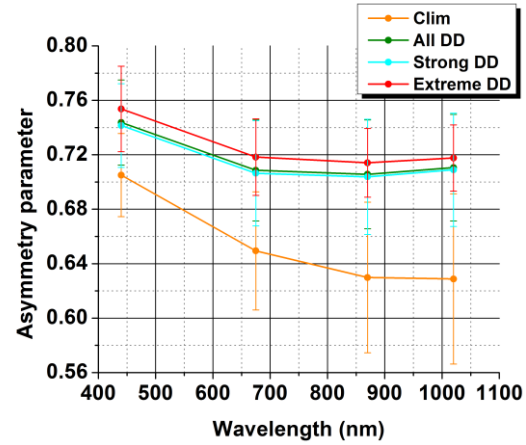


(ii)

**Figure S3:** Boxplots of AERONET: (i)  $\alpha_{440-870nm}$  and (ii)  $r_{eff}$  retrievals calculated from all the available data (orange color) as well as from the corresponding measurements for all intense (green color), strong (cyan color) and extreme (red color) desert dust episodes identified over the Mediterranean, during the period Mar. 2000 – Feb. 2013.

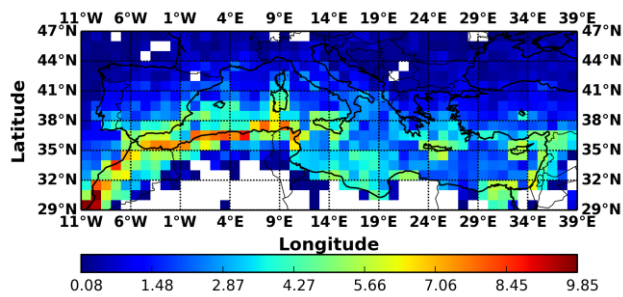


(i)

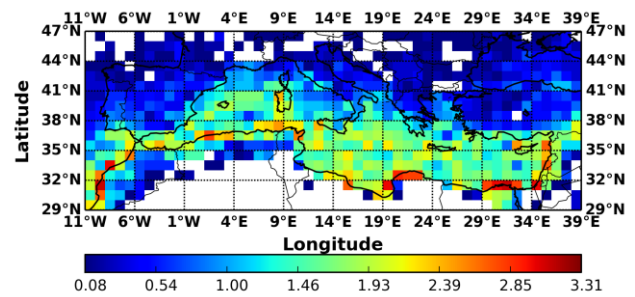


(ii)

**Figure S4:** Spectral variation of the averaged: (i) single scattering albedo and (ii) asymmetry parameter retrievals, provided by the AERONET database, for the whole study period (orange curve) as well as for all (green curve), strong (cyan curve) and extreme (red curve) dust episodes, identified over the Mediterranean, during the period Mar. 2000 – Feb. 2013. The error bars represent the calculated standard deviations.

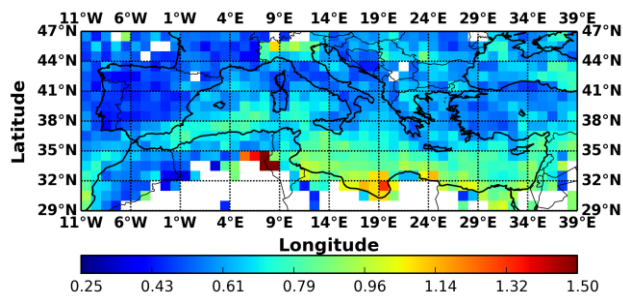


(i)

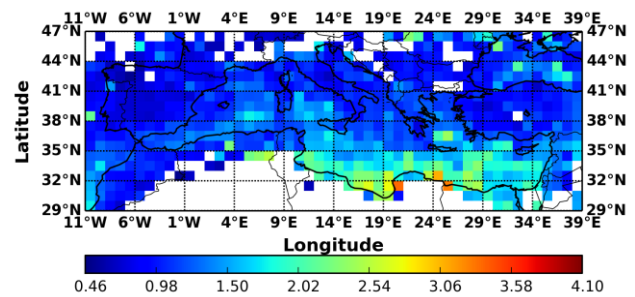


(ii)

**Figure S5:** Geographical distributions of the frequency of occurrence (episodes yr<sup>-1</sup>) of: (i) strong and (ii) extreme desert dust episodes, for the period 2003 – 2012 (MODIS-Terra), over the broader area of the Mediterranean basin.

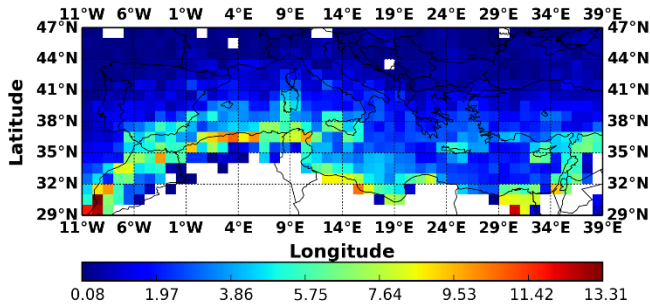


(i)

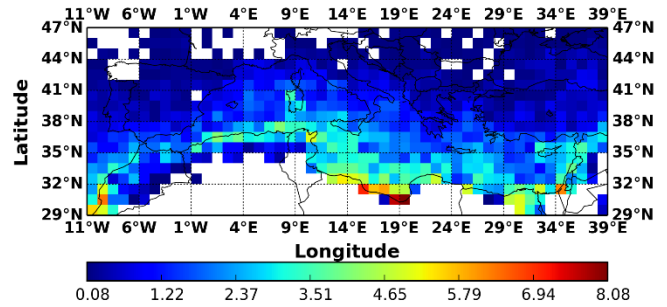


(ii)

**Figure S6:** Geographical distributions of the intensity (in terms of  $AOD_{550nm}$ ) of: (i) strong and (ii) extreme desert dust episodes, for the period 2003 – 2012 (MODIS-Terra), over the broader area of the Mediterranean basin.

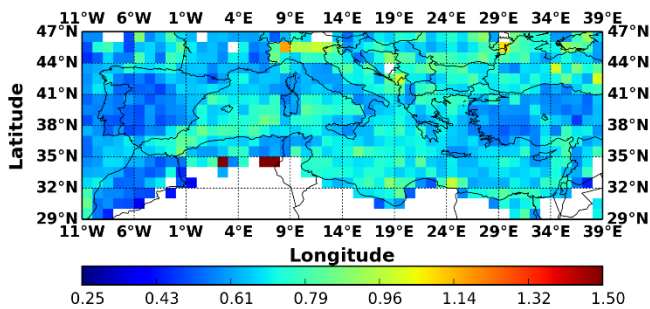


(i)

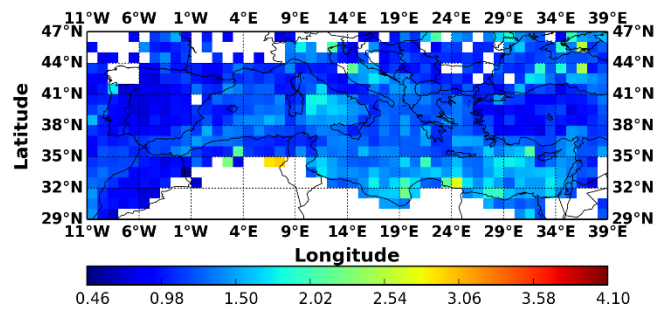


(ii)

**Figure S7:** Geographical distributions of the frequency of occurrence (episodes yr<sup>-1</sup>) of: (i) strong and (ii) extreme desert dust episodes, for the period Mar. 2000 – Feb. 2013, over the broader area of the Mediterranean basin, calculated according to METHOD-B, based on MODIS-Terra retrievals.

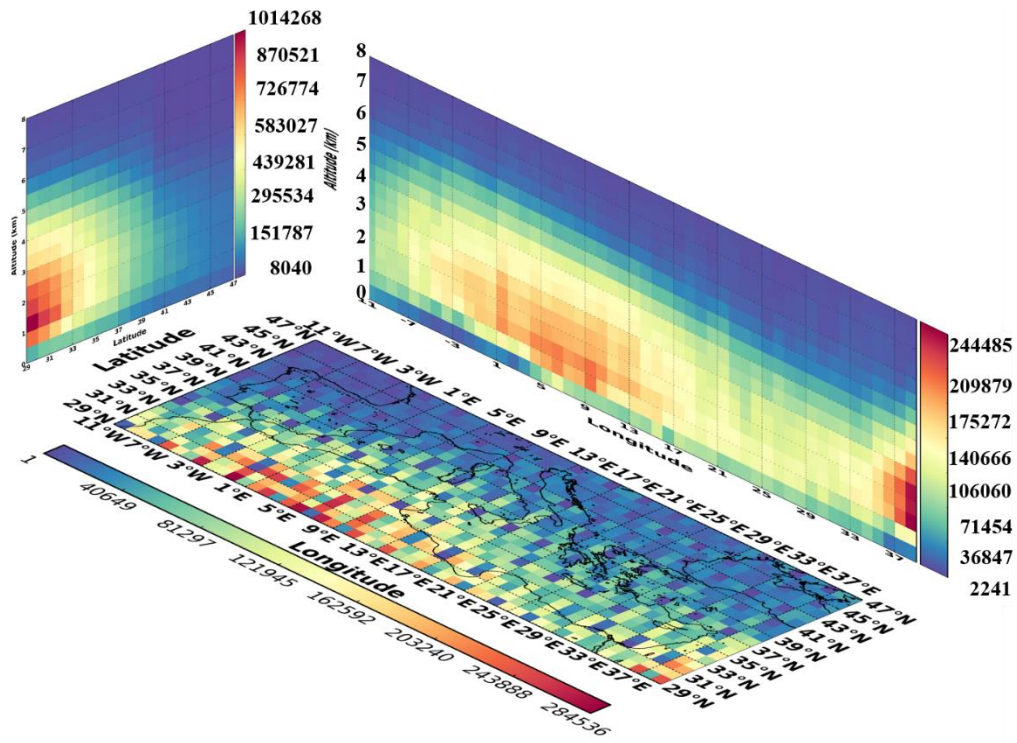


(i)

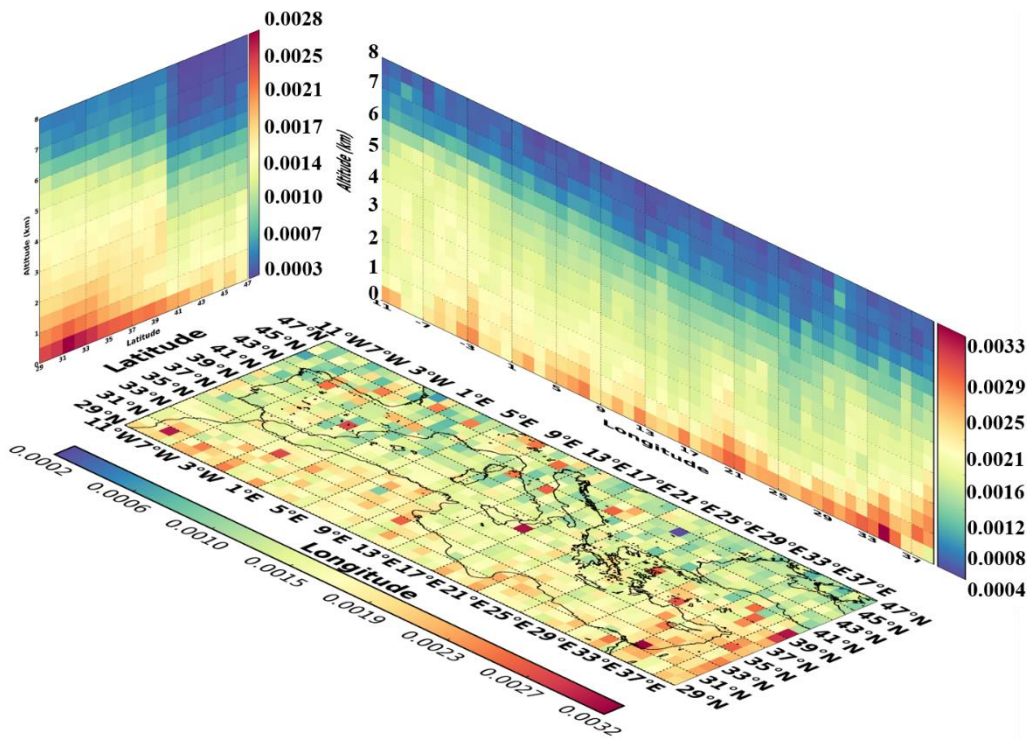


(ii)

**Figure S8:** Geographical distributions of the intensity (in terms of  $AOD_{550nm}$ ) of: (i) strong and (ii) extreme desert dust episodes, for the period Mar. 2000 – Feb. 2013, over the broader area of the Mediterranean basin, calculated according to METHOD-B, based on MODIS-Terra retrievals.

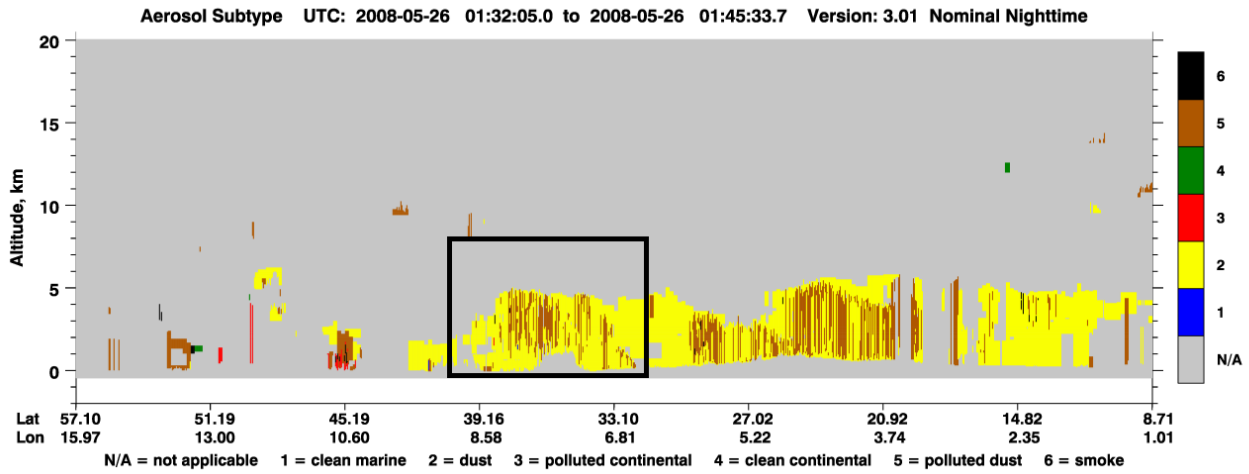


(i)

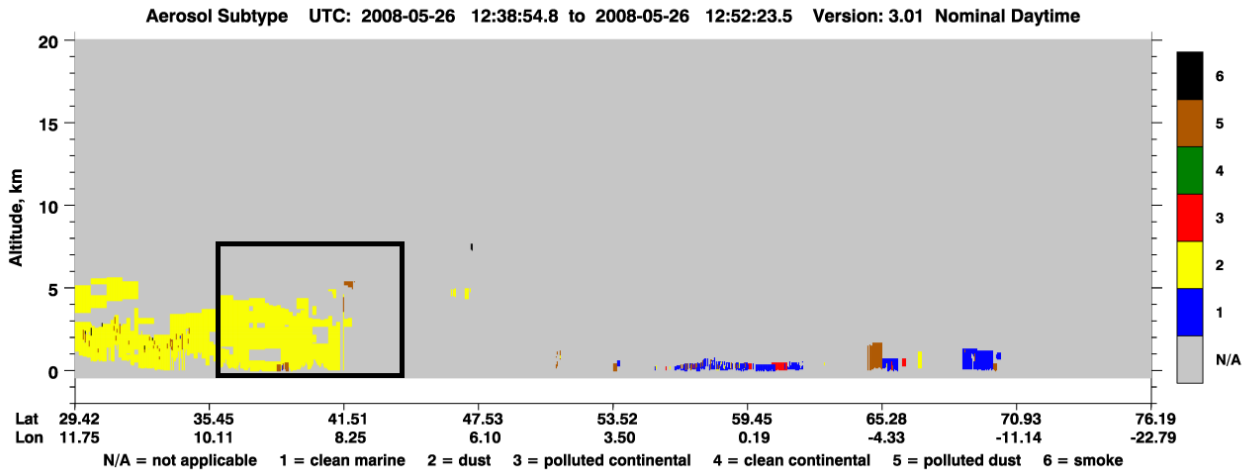


(ii)

**Figure S9:** Three dimensional structure of the: (i) overall number of dust and polluted dust observations and (ii) total backscatter coefficient at 532 nm (in  $\text{km}^{-1} \text{sr}^{-1}$ ), over the broader Mediterranean basin, based on CALIOP-CALIPSO vertically resolved retrievals for the period Jun. 2006 – Feb. 2013.

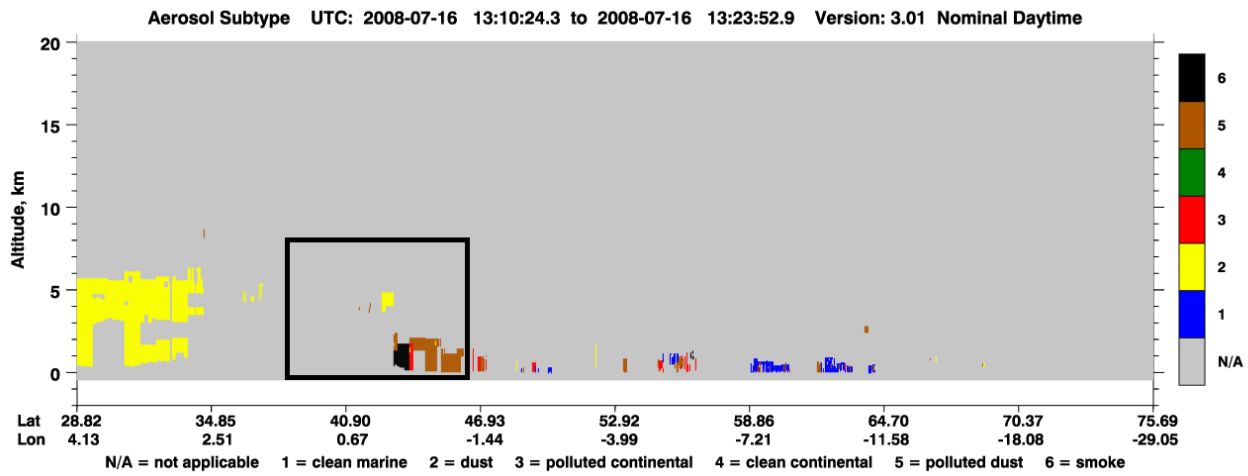


(i)

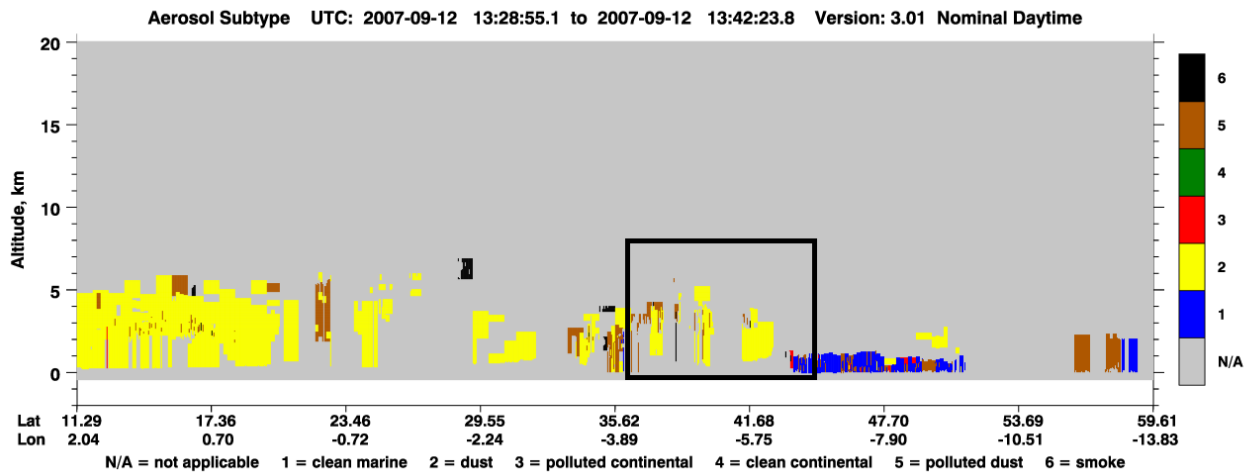


(ii)

**Figure S10:** Cross sections of the aerosol subtype profiles along the CALIOP-CALIPSO track during: (i) nighttime and (ii) daytime, on 26<sup>th</sup> May 2008, over the station Censt (Lat: 39.064, Lon: 8.457). The rectangles represent the part of the CALIOP-CALIPSO track depicted in Figure 10.



(i)



(ii)

**Figure S11:** Cross sections of the aerosol subtype profiles along the CALIOP-CALIPSO track during daytime over the stations: (i) Els Torms (Lat: 41.395, Lon: 0.721) on 16<sup>th</sup> July 2008 and (ii) San Pablo (Lat: 39.525, Lon: -4.353) on 12<sup>th</sup> September 2007. The rectangles represent the part of the CALIOP-CALIPSO track depicted in Figure 11.

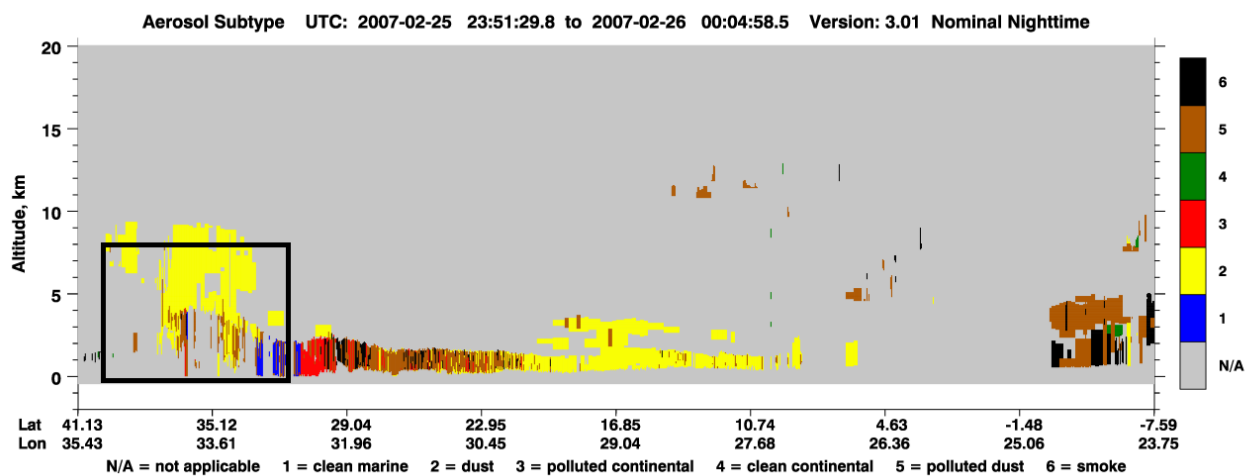


**Figure S12:** Cross section of the aerosol subtype along the CALIOP-CALIPSO track during nighttime over the station Agia Marina (Lat: 35.039, Lon: 33.058) on 25<sup>th</sup> February 2007. The rectangular represents the part of the CALIOP-CALIPSO track depicted in Figure 12.